A reversible, p53-dependent G_0/G_1 cell cycle arrest induced by ribonucleotide depletion in the absence of detectable DNA damage

Steven P. Linke,[1,2] Kristie C. Clarkin,[1] Aldo Di Leonardo,[1,3] Amy Tsou,[4] and Geoffrey M. Wahl[1,5]

[1]Gene Expression Lab, The Salk Institute, La Jolla, California 92037 USA; [2]Department of Biology, University of California–San Diego, La Jolla, California 92037 USA; [3]Department of Cell and Developmental Biology, University of Palermo, Palermo, Italy; [4]Molecular Biology and Virology Lab, The Salk Institute, La Jolla, California 92037 USA

Cells with a functional p53 pathway undergo a G_0/G_1 arrest or apoptosis when treated with γ radiation or many chemotherapeutic drugs. It has been proposed that DNA damage is the exclusive signal that triggers the arrest response. However, we found that certain ribonucleotide biosynthesis inhibitors caused a p53-dependent G_0 or early G_1 arrest in the absence of replicative DNA synthesis or detectable DNA damage in normal human fibroblasts. CTP, GTP, or UTP depletion alone was sufficient to induce arrest. In contrast to the p53-dependent response to DNA damage, characterized by long-term arrest and irregular cellular morphologies, the antimetabolite-induced arrest was highly reversible and cellular morphologies remained relatively normal. Both arrest responses correlated with prolonged induction of p53 and the Cdk inhibitor $p21^{WAF1/CIP1/SDI1}$ and with dephosphorylation of pRb. Thus, we propose that p53 can serve as a metabolite sensor activated by depletion of ribonucleotides or products or processes dependent on ribonucleotides. Accordingly, p53 may play a role in inducing a quiescence-like arrest state in response to nutrient challenge and a senescence-like arrest state in response to DNA damage. These results have important implications for the mechanisms by which p53 prevents the emergence of genetic variants and for developing more effective approaches to chemotherapy based on genotype.

[*Key Words*: p53; $p21^{WAF1/CIP1/SDI1}$; pRb; normal human diploid fibroblasts; antimetabolites; cell cycle control]

Received November 28, 1995; revised version accepted March 1, 1996.

The tumor suppressor p53 is an important factor for maintaining genetic stability. It is a cell cycle checkpoint protein that helps regulate progression from G_1 into S phase. Many environmental insults and cancer treatments, including γ radiation and chemotherapeutic drugs, increase p53 levels, leading to a G_1 phase cell cycle arrest or apoptosis (Kastan et al. 1991; Kuerbitz et al. 1992; Livingstone et al. 1992; Yin et al. 1992; Clarke et al. 1993; Lowe et al. 1993a,b; Di Leonardo et al. 1994). The G_1 arrest pathway probably involves p53-dependent transcriptional activation of $p21^{WAF1/CIP1/SDI1}$ (p21) (El-Deiry et al. 1994). p21 inhibits G_1 cyclin–Cdk complexes, such as cyclin D–Cdk4/Cdk6 and cyclin E–Cdk2 (Harper et al. 1993; Xiong et al. 1993). Whereas p21 levels increase reversibly in quiescent cells, they increase irreversibly in senescent cells (Noda et al. 1994). Inhibition of G_1 cyclin–Cdk complexes, in turn, inhibits phosphorylation of pRb (Harper et al. 1993; Dulic et al. 1994), thereby preventing activation of E2F-responsive G_1/S transition genes such as dihydrofolate reductase (DHFR) and thymidylate synthase (TS) (for review, see Farnham et al. 1993; Almasan et al. 1995b). It is also likely that other uncharacterized factors downstream of p53 are involved in the arrest response. Thus, p53 helps maintain genetic stability by preventing progression into S phase under adverse conditions, such as those created by environmental stresses or treatment with anticancer agents.

γ radiation and DNA-interactive drugs (e.g., DNA strand-breakage agents and DNA topoisomerase II inhibitors) cause DNA damage directly and can generate a p53-dependent G_1 arrest (Kastan et al. 1991, 1992; Kuerbitz et al. 1992). Consistent with these studies, DNA strand breaks have been shown to be sufficient to induce p53 and cell cycle arrest (Nelson and Kastan 1994; Huang et al. 1996). Previously, we found that normal human diploid fibroblasts (NDFs) undergo a prolonged, probably permanent arrest similar to senescence in response to γ radiation-induced DNA damage (Di Leonardo et al. 1994). These data indicate that p53 helps

[5]Corresponding author.

maintain genetic stability in human fibroblasts by preventing replication of damaged DNA through a prolonged G_0/G_1 arrest.

There is evidence that p53 can also be activated in the absence of DNA damage (Hupp et al. 1995) and may respond to metabolic signals. Whereas many p53-responsive anticancer agents cause DNA damage directly, antimetabolites such as the CAD inhibitor *n*-phosphonacetyl-L-aspartate (PALA) (Collins and Stark 1971) (Fig. 1) primarily disrupt nucleotide pools. Cells with a functional p53 pathway ($p53^+$) arrest in G_1 in the presence of PALA, whereas cells lacking a functional pathway ($p53^-$) are able to progress into S phase (Livingstone et al. 1992; Yin et al. 1992). Unlike the prolonged arrest seen in γ-irradiated cells, PALA-treated $p53^+$ cells remain capable of dividing (Livingstone et al. 1992; Di Leonardo et al. 1993b). This suggests that p53 can also help maintain genetic stability by preventing DNA replication during metabolic depletion.

In responding to the metabolic depletion created by antimetabolites, p53 could be acting as a nucleotide sensor analogous to nutrient sensors in yeast. Yeast contain a G_1 checkpoint function that prevents progression from G_1 into S phase during nutritional depletion (for review, see Nasmyth 1993). A nucleotide sensor in mammalian cells could prevent replication when DNA precursor pools are low. This is significant because elongation of S phase during nucleotide depletion has been associated with increased chromosome breakage, probably precipitated by inhibition of replication fork progression (for discussion and references, see Windle et al. 1991; Di Leonardo et al. 1993b). Such breaks can occur frequently at chromosome fragile sites, that may provide the initial lesions required for gene amplification, one form of genetic instability (Windle et al. 1991; Ma et al. 1993; Bertoni et al. 1994; Kuo et al. 1994; Ishizaka et al. 1995). Thus, DNA damage is a secondary effect of antimetabolites that probably requires transit through S phase. A nucleotide sensor in G_1, therefore, would help preserve genetic stability by preventing progression into S phase under conditions favorable for DNA damage and gene amplification.

Here, we study whether nucleotide depletion can activate a DNA damage-independent arrest mechanism mediated by p53. We show that the G_0/G_1 arrest induced by treatment with certain ribonucleotide biosynthesis inhibitors (Fig. 1) is different from that induced by γ radiation, indicating the existence of an alternate p53-dependent arrest function. This function may help maintain genetic stability by preventing progression from G_1 into S phase during metabolic depletion.

Results

Cell cycle effects of anticancer agents on G_0-synchronized and asynchronous $p53^+$ and $p53^-$ cells

Previous studies have shown that p53 mediates a G_1 arrest in many cell types following treatment with a number of direct DNA-damaging agents and the antimetabolite PALA. As a result, it is generally accepted that DNA damage is the exclusive upstream signal that leads to p53-mediated arrest. However, although antimetabolites like PALA can cause DNA damage during progression through S phase, the kinetics of the PALA-induced arrest in asynchronous cultures suggests that a majority of the arrested cells do not progress through S phase prior to stopping in G_0/G_1. Therefore, we tested the ability of PALA and a variety of other antimetabolites that disrupt nucleotide pools (Fig. 1) to maintain G_0-synchronized $p53^+$ (WS1neo and NHF-3neo) and $p53^-$ (WS1E6 and NHF-3E6) NDF in G_0/G_1. Treatment of G_0-synchronized cells minimized the possibility of replication-associated DNA damage contributing to the arrest. The thymidine analog bromodeoxyuridine (BrdU) was added at the time of release for continuous labeling of DNA until harvest, except as noted for fluorouracil (5-FU) and methotrexate (MTX). This method allowed detection of any cell that entered S phase over the entire release period and enabled monitoring of cells that did not arrest in the initial G_0/G_1 as they progressed through subsequent phases. Results for G_0 synchrony by contact inhibition and serum deprivation were equivalent. Similar results were also achieved in a variety of asynchronously-treated $p53^+$ and $p53^-$ cell lines and strains as summarized in Table 1. Antimetabolite concentrations ranged from ~9 to 90 times the IC_{50} of the cells (concentration that inhibits proliferation by 50%), and γ radiation doses ranged from 1 to 8 Gy.

Although the percentages of cells in each phase varied for each treatment and cell type, the dot plots shown in Figures 2 and 3, A–F, for WS1neo and WS1E6 cells are representative of all $p53^+$ and $p53^-$ cells tested in this study. Figure 2, A and I, shows serum-deprived populations, which typically contained <3% $BrdU^+$ cells. Figure 2, B and J, depicts characteristic profiles of untreated cells labeled continuously with BrdU for 72 hr after release in complete medium.

Inhibitors of UMP and GMP biosynthesis cause a p53-dependent G_0/G_1 arrest

Consistent with previous reports (Kastan et al. 1991; Kuerbitz et al. 1992; Livingstone et al. 1992; Yin et al. 1992), γ radiation and PALA caused a p53-dependent G_0/G_1 cell cycle arrest in asynchronous cultures (Table 1). $p53^-$ cells accumulated in S phase during PALA treatment, presumably because of depletion of nucleotide precursors, whereas little change in the fraction of S phase cells was seen after γ irradiation. PALA treatment also prevented progression of G_0-synchronized $p53^+$ cells into S phase. In contrast, $p53^-$ cells accumulated in S phase when released in PALA (e.g., Fig. 2, cf. C and K). Few $p53^-$ cells reached the subsequent G_1 after release, indicating that their rate of progression through S phase was substantially reduced by these treatments. Similar results were obtained after treatment with the UMP synthase (UMP-S) inhibitor pyrazofurin (Pyf) (Cadman et al. 1978) (Table 1; data not shown for G_0-synchronized cultures) and the IMP-dehydrogenase (IMP-D) inhibitors mycophenolic acid (MA) (Cohen and Sadee 1983) (Table

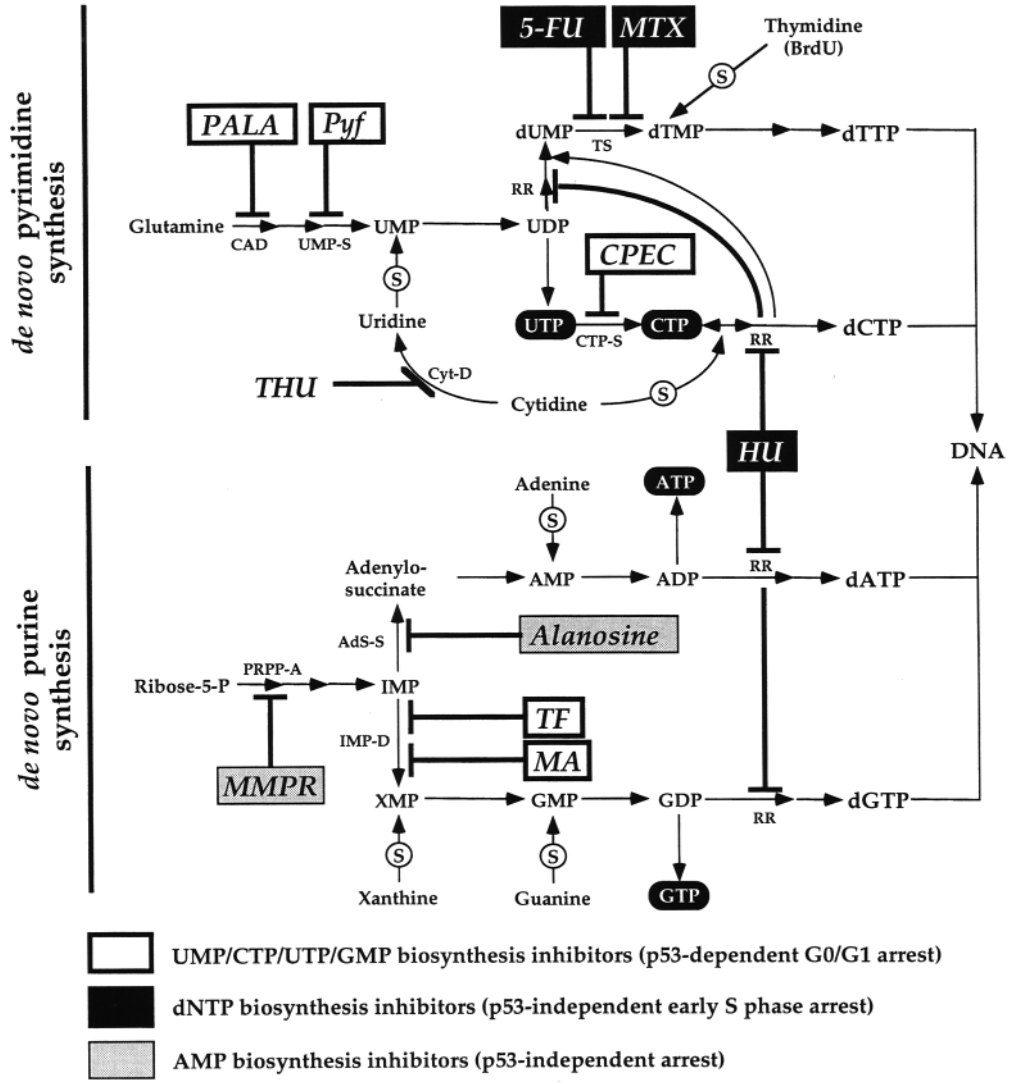

Figure 1. De novo pyrimidine and purine nucleotide synthetic pathway. Arrows denote steps in de novo nucleotide biosynthesis. Circled S's depict salvage pathways. Nucleotides in dark ovals are ribonucleotide triphosphates (rNTPs). Antimetabolites are indicated by italics, and their points of action are symbolized with T-bars adjacent to the primary enzyme that is inhibited. White boxes contain UMP, CTP, UTP, and GMP biosynthesis inhibitors that induce a p53-dependent G_0/G_1 arrest. Dark boxes contain dNTP biosynthesis inhibitors that induce a p53-independent early S phase arrest. (In addition to inhibiting biosynthesis of dTMP/dTTP, MTX also inhibits early purine biosynthesis. However, the purine inhibition made only a small contribution to cell cycle arrest.) Gray boxes contain AMP biosynthesis inhibitors that cause other types of p53 – independent arrest. (Although MMPR is thought to inhibit an early step in pyrimidine synthesis, its primary rNTP effect was depletion of ATP pools.) Enzymes: (AdS-S) adenylosuccinate synthase; (CAD) carbamoyl phosphate synthase/aspartate carbamoyltransferase/dihydroorotase; (CTP-S) cytidine triphosphate synthase; (Cyt-D) cytidine deaminase; (IMP-D) inosine monophosphate dehydrogenase; (PRPP-A) phosphoribosylpyrophosphate amidotransferase; (RR) ribonucleotide reductase; (TS) thymidylate synthase; (UMP-S) uridine monophosphate synthase (two components). Antimetabolites: (CPEC) cyclopentenylcytosine; (5-FU) fluorouracil; (HU) hydroxyurea; (MMPR) 6-methyl mercaptopurine riboside; (MTX) methotrexate; (MA) mycophenolic acid; (PALA) *n*-phosphonacetyl-L-aspartate; (Pyf) pyrazofurin; (TF) tiazofurin; (THU) tetrahydrouridine.

1; Fig. 2D,L) and tiazofurin (TF) (Cooney et al. 1982) (Table 1; data not shown for G_0-synchronized cultures). In the G_0-synchronized cultures treated with these drugs, <10% of $p53^+$ cells entered S phase during the entire labeling period, whereas >85% of $p53^-$ cells progressed into and accumulated in S phase relative to the untreated control. These results agree with recent findings for PALA treatment of G_0-synchronized wild-type and $p53^{-/-}$ mouse embryo fibroblasts (MEFs) (Deng et al. 1995) and parental WS1 and LFS-041 cells (Di Leonardo et al. 1993b). Thus, the ability of cells to progress from G_0/G_1 into S phase during treatment with inhibitors of UMP or GMP biosynthesis is dependent on the presence of a functional p53 pathway.

Table 1. *Summary of cell cycle effects of anticancer agents on asynchronous p53⁺ and p53⁻ cells*

Cell strain/ line	p53 status	γ (1–8 Gy)	PALA (100–500 μM)	Pyf (2–10 μM)	MA (2–10 μM)	HU (1–5 mM)	5-FU (0.5–5 μM)	MTX (0.1–1 μM)	Alanosine (20–100 μM)	MMPR (2–10 μM)
WS1	wt	G_0/G_1	G_0/G_1	G_0/G_1	G_0/G_1	early S	early S	early S	S	
WS1neo	wt	G_0/G_1	G_0/G_1	G_0/G_1	G_0/G_1	early S	early S	early S	S	G_0/G_1
NHF-3	wt	G_0/G_1	G_0/G_1	G_0/G_1	G_0/G_1		early S	early S	S	
NHF-3neo	wt	G_0/G_1	G_0/G_1	G_0/G_1	G_0/G_1			early S	S	G_0/G_1
WI-38	wt	G_0/G_1	G_0/G_1							
WI-38neo	wt	G_0/G_1	G_0/G_1					early S		
RPE-h	wt	G_0/G_1	G_0/G_1							
RPE-hneo	wt	G_0/G_1	G_0/G_1					early S		
IMR-90	wt		G_0/G_1	G_0/G_1	G_0/G_1	early S	early S	early S	S	
WS1E6	degraded	no arrest	S	S	S	early S	early S	early S	S	G_0/G_1
NHF-3E6	degraded	no arrest	S	S	S			early S	S	G_0/G_1
WI-38E6	degraded	no arrest	S					early S		
RPE-hE6	degraded	no arrest	S							
LFS-087	NF[a]		S		S			early S		
LFS-041	NF[b]		S	S	S	early S	early S	early S	S	
H1299	NF[c]	no arrest	S	S	S			early S	S	

Asynchronous cultures were treated with the indicated agent for 24–72 hr at the doses shown, pulse-labeled in 10 μM BrdU for 30 min, fixed, stained with propidium iodide and anti-BrdU–FITC, and analyzed by flow cytometry. The resultant cell cycle profiles are summarized as no arrest, G_0/G_1 arrest (G_0/G_1), accumulation in S phase (S), or arrest in early S phase (early S). (wt) Wild-type p53; (degraded) p53 degradation by ubiquitin pathway because of E6 expression; (NF) nonfunctional.
[a]Point mutation changing codon 248 from Arg → Trp.
[b]Frameshift deletion in codon 184 (Yin et al. 1992).
[c]Intragenic deletion of 5′ end (Bodner et al. 1992).

The p53-dependent G_0/G_1 arrest induced by PALA or Pyf is reversible

We showed previously that the p53-dependent G_0/G_1 arrest caused by γ radiation-induced DNA damage was prolonged and probably permanent (Di Leonardo et al. 1994). The reversibility of the antimetabolite-induced arrest was determined by adding metabolites that restored nucleotide levels through salvage pathways (Fig. 1). The G_0/G_1 arrest induced in p53⁺ cells and the S phase ac-

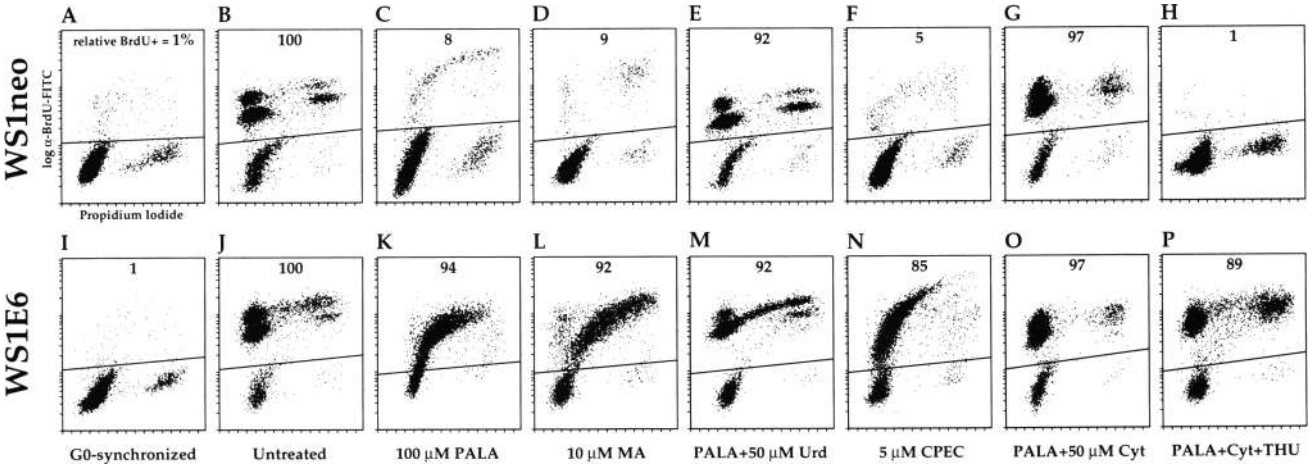

Figure 2. Cell cycle effects of UMP, CTP, UTP, and GMP biosynthesis inhibitors on G_0-synchronized p53⁺ and p53⁻ cells. G_0-synchronized cultures were treated with the indicated agents and released in medium containing BrdU for continuous DNA labeling. After 72 hr, cells were stained with propidium iodide and anti-BrdU–FITC and analyzed by flow cytometry. Concentrations of events with a 2N DNA content indicate G_0/G_1 phase cells, concentrations of events with a 4N DNA content indicate G_2/M phase cells, and events intermediate between 2N and 4N indicate S phase cells. Events below the horizontal line represent cells that remained arrested in the initial G_0/G_1 after release, and events above the horizontal line represent cells that entered the cycle and incorporated BrdU after release. Multiple layers of BrdU⁺ events in unarrested cultures indicate cells that incorporated BrdU during S phase following release, then divided and progressed through additional cycles. Numbers represent the percentage of cells that escaped from the initial G_0/G_1 after release relative to the untreated controls (relative BrdU⁺). BrdU⁺ cells in the untreated controls were 77% and 81%, respectively, for WS1neo and WS1E6 in the representative experiment shown. Percentages are normalized to the starting population (i.e., events in the second G_1, S, and G_2/M phases were divided by two, and those in the third were divided by four).

cumulation induced in p53$^-$ cells by treatment with PALA or Pyf were prevented by cotreatment with the salvage metabolite uridine at a concentration of 50 μM. The cell cycle profiles of both asynchronous and G_0-synchronized cotreated cultures were nearly indistinguishable from the untreated control, although the G_2/M populations were slightly higher (e.g., Fig. 2E,M). The PALA- or Pyf-induced arrest responses were not affected by cotreatment with thymidine or purine salvage metabolites, and cotreatment of γ-irradiated cells with salvage metabolites did not affect cell cycle progression. The arrest responses induced by MA or TF were similarly reversible by cotreatment with the salvage metabolites guanosine (10 μM) and xanthine (10 μM) (data not shown).

Depletion of CTP or UTP alone is sufficient to induce a p53-dependent G_0/G_1 arrest

Because PALA and Pyf reduce both CTP and UTP levels, we tested drug combinations that reduced each pool selectively. The CTP synthase (CTP-S) inhibitor cyclopentenylcytosine (CPEC) depletes CTP (Moyer et al. 1986). G_0-synchronized WS1neo cells released in the presence of 2–10 μM CPEC remained in G_0/G_1, whereas WS1E6 cells progressed into and accumulated in S phase, similar to their response to PALA (Fig. 2F,N). Cells cotreated with PALA and 50 μM cytidine did not arrest (Fig. 2G,O). This result was identical to that obtained by cotreatment with uridine and was expected, as cellular cytidine deaminases convert cytidine to uridine and restore both UTP and CTP pools (Fig. 1). However, treatment with a combination of PALA (100 μM), cytidine (50 μM), and the cytidine deaminase (Cyt-D) inhibitor tetrahydrouridine (THU) (Cadman and Benz 1980) at 100 μM selectively depleted UTP pools (see below). WS1neo cells remained in G_0/G_1 when treated with this combination, but WS1E6 cells progressed into S phase (Fig. 2H,P). Although the accumulation of p53$^-$ cells in the first S phase was not as profound with this drug combination as with other treatments, the cells progressed significantly more slowly than untreated cells. Less than 5% of the cells had progressed beyond the second cycle compared with >50% in the untreated control (data not shown). This suggests that sole depletion of UTP may have less of an effect on entry into or progression through the first S phase than depletion of other rNTPs or combinations of rNTPs. WS1neo cells treated with PALA, uridine, and THU did not arrest, which is consistent with the ability of uridine to restore both UTP and CTP without the need for cytidine deaminases. In addition, THU treatment alone had no effect on cell cycle progression (data not shown). These data indicate strongly that sole depletion of CTP- or UTP-derived metabolites can cause a p53-dependent G_0/G_1 arrest.

dNTP biosynthesis inhibitors cause a p53-independent accumulation of cells in early S phase

In contrast to the CTP, UTP, and GMP biosynthesis inhibitors, treatment of both p53$^+$ and p53$^-$ asynchronous cultures with the ribonucleotide reductase (RR) inhibitor hydroxyurea (HU) (Skoog and Nordenskjold 1971), the TS inhibitor 5-FU (Santi et al. 1974), or the DHFR and TS inhibitor MTX (see below and Moran et al. 1979) caused an early S phase arrest (Table 1). The cell cycle effects of both 5-FU and MTX were prevented almost completely by cotreatment with the salvage metabolite thymidine or the thymidine analog BrdU (data not shown). Because BrdU acts as a salvage metabolite for these drugs during continuous labeling, a 30-min pulse was used instead. Both WS1neo and WS1E6 cells released from G_0 synchrony for 24–96 hr in the presence of 5-FU, MTX, and HU showed a significant accumulation of BrdU$^+$ cells above the G_1 subpopulation (e.g., Fig. 3, A and D, shows MTX at 72 hr). This indicates that cells were arrested in the early stages of replication, presumably caused by depletion of thymidine precursors, and that replenishment of the dTTP pool enabled progression into very early S phase during the 30-min BrdU labeling. Cotreatment of 5-FU- and MTX-treated cells with purine salvage metabolites did not reverse the S phase arrest (data not shown). This indicates that the primary cause of cell cycle inhibition for 5-FU and MTX under these conditions is through depletion of dTTP, although MTX can inhibit purine biosynthesis under other circumstances. These data suggest that cells are able to progress through G_1 to the G_1/S boundary or into early S phase during treatment with antimetabolites that primarily affect dNTP biosynthesis, regardless of p53 status.

Cell cycle effects of AMP biosynthesis inhibitors

In asynchronous cultures, the adenylosuccinate synthase (AdS-S) inhibitor alanosine (Gale and Schmidt 1968) caused an accumulation of both p53$^+$ and p53$^-$ cells in S phase (e.g., Fig. 3B,E; Table 1). The PRPP amidotransferase (PRPP-A) inhibitor 6-methylmercaptopurine riboside (MMPR) (Henderson and Patterson 1973), which affected primarily ATP pools (see below), caused a G_0/G_1 arrest in both p53$^+$ and p53$^-$ cells (e.g., Fig. 3C,F; Table 1). Treatment of G_0-synchronized cultures with alanosine and MMPR had similar effects to those observed in asynchronous cultures (data not shown).

Timing of release from PALA arrest resembles that of quiescent cells

The reversibility of the PALA-induced arrest resembled quiescence. Therefore, we compared the timing of S phase entry in PALA-arrested cells versus cells synchronized in G_0 by contact inhibition or serum deprivation. Cells were synchronized in G_0 and released for 24 hr in 100 μM PALA and 65 μM BrdU (for continuous labeling) (Fig. 3G). The length of time required for cells to enter S phase and the efficiency of the reversal from the PALA block was determined by releasing cells in 50 μM uridine and 65 μM BrdU and harvesting them at various times thereafter. Cells began incorporating BrdU ~14 hr after addition of uridine (Fig. 3H), about the same time as contact-inhibited cells and a few hours before serum-

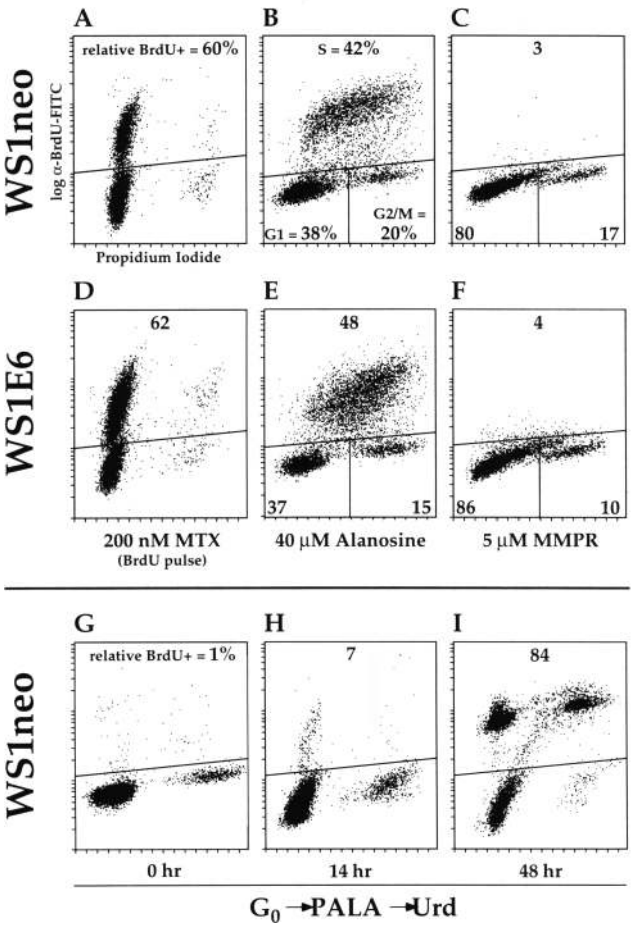

Figure 3. Cell cycle effects of dNTP and AMP biosynthesis inhibitors, and kinetics of release from PALA-induced arrest. (*A–F*) Cells were pulse-labeled with BrdU for 30 min after 72 hr of treatment with the indicated agent. (*A,D*) G_0-synchronized cultures released in 200 nM MTX. Numbers represent the percentage of cells that escaped from the initial G_0/G_1 after release relative to the untreated controls (relative BrdU$^+$). (*B,C,E,F*) Asynchronous cultures treated with the indicated agent. Numbers indicate the percentage of cells in each cell cycle phase as shown in *B*. (*G*) G_0-synchronized cells released in medium containing 100 μM PALA and 65 μM BrdU for 24 hr. (*H*) PALA-arrested cells released for 14 hr in 50 μM uridine and 65 μM BrdU. (*I*) PALA-arrested cells released for 48 hr. All cells were stained with propidium iodide and anti-BrdU-FITC and analyzed by flow cytometry.

deprived cells began incorporating BrdU following release (data not shown). Greater than 80% of PALA-arrested cells released in uridine entered S phase relative to cells released from serum deprivation within 48 hr (Fig. 3I). Addition of uridine to asynchronous WS1 or WS1neo cultures treated for 48–96 hr with 100 μM PALA or 10 μM Pyf also rescued the cells from arrest. Cells began incorporating BrdU ~18 hr after addition of uridine, a few hours later than seen after release from serum deprivation. The efficiency of release from the PALA-induced arrest in these cells was slightly lower than in the presynchronized cells (~60%–70% relative to cells released from serum deprivation). This suggests that addition of PALA to asynchronous cultures can reduce their plating efficiency, presumably because of the DNA damage incurred by a subset of cells that traversed multiple S phases during treatment. Also, the release was less synchronous than for G_0-synchronized cells; large numbers of cells were still entering S phase from the initial G_0/G_1 after 48 hr (data not shown). Taken together, these data suggest that UMP depletion causes cells to enter a largely reversible, p53-dependent G_0-like state.

Effects of PALA and γ radiation on morphology and p53 localization in NDF

We treated asynchronous WS1 cells with 100 μM PALA or 4 Gy γ radiation to determine whether the arrested cells exhibited differences in morphology and/or p53 localization. Cells were fixed, stained with a p53-specific antibody, processed for immunofluorescence, and photographed 3, 12, 24, and 96 hr after treatment (24 and 96 hr time points shown in Fig. 4). PALA-treated cells maintained normal morphologies through at least 24 hr and had become only slightly enlarged at 96 hr, consistent with the typical morphology of quiescent WS1 cells. Induction of p53 in the nucleus was noticeable by 12 hr and remained high through 96 hr. In contrast, γ-irradiated cells began enlarging within 12 hr and exhibited the enlarged, flattened morphology of senescent fibroblasts by 96 hr, as we reported previously (Di Leonardo et al. 1994). Induction of p53 in the nucleus was noticeable within 3 hr and remained high through 96 hr. Untreated cells continued growing and did not show significant nuclear p53 staining.

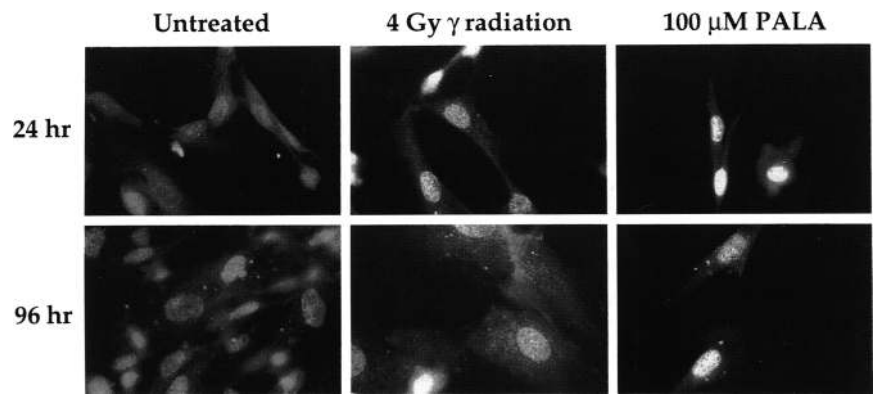

Figure 4. Effects of PALA and γ radiation on cellular morphology and p53 localization. WS1neo cells were treated and fixed at the indicated times, and then stained with anti-p53 DO-1 (Ab-6). Cells were photographed at 100× magnification.

The effects of antimetabolites on nucleotide pools are the same in p53$^+$ and p53$^-$ cells

Because p53 might influence nucleotide biosynthesis by affecting E2F activity through factors such as pRb phosphorylation (see below), we tested whether p53$^-$ cells failed to arrest as a result of the inability of the drugs to deplete nucleotide pools to the same degree as in p53$^+$ cells. Asynchronous WS1neo and WS1E6 cells were treated for 3–24 hr with antimetabolites, and ribonucleotide triphosphate (rNTP) levels were assayed by HPLC (a majority of cells were arrested by 24 hr if the antimetabolite induced arrest). No significant differences in overall pool sizes or the magnitude of depletion were seen in rNTP levels between WS1neo and WS1E6 cells with any of the treatments. Consistent with previous reports (Moyer et al. 1982), PALA (100 μM) and Pyf (10 μM) caused substantial reductions in UTP and CTP levels (to <10% of the untreated controls), whereas ATP and GTP levels increased slightly in both WS1neo and WS1E6 cells (Fig. 5A,B). Levels of UTP-activated carbohydrates, including UDP–glucose and UDP–galactose, were also substantially reduced (data not shown). Similar results were obtained in NHF-3 cells and in WS1 cells released from G_0 synchrony (data not shown). MA (10 μM) and TF (100 μM) reduced GTP levels to ~20% of the controls. These drugs also caused slight decreases in ATP and slight increases in UTP and CTP levels. Also consistent with previous studies (Moyer et al. 1982), rNTP analysis revealed that UTP and CTP pools were restored and somewhat elevated in cultures cotreated with PALA and uridine. Treatment with PALA (100 μM), cytidine (50 μM), and THU (100 μM) selectively depleted UTP pools to <10% of controls. In line with their specificity for dNTP biosynthesis, 5-FU (1 μM) and HU (1 mM) had no appreciable effects on rNTP pool levels. MTX (200 nM) caused moderate reductions in ATP and GTP levels (to ~70% of control) and moderate increases in UTP and CTP levels (data not shown). Alanosine (20 μM) reduced ATP to ~30% of control cells and caused increases in UTP, CTP, and GTP levels. Similar to alanosine, the predominant rNTP pool effect of MMPR (5 μM) was a decrease in ATP (to ~60% of controls), whereas UTP, CTP, and GTP levels all increased modestly (data

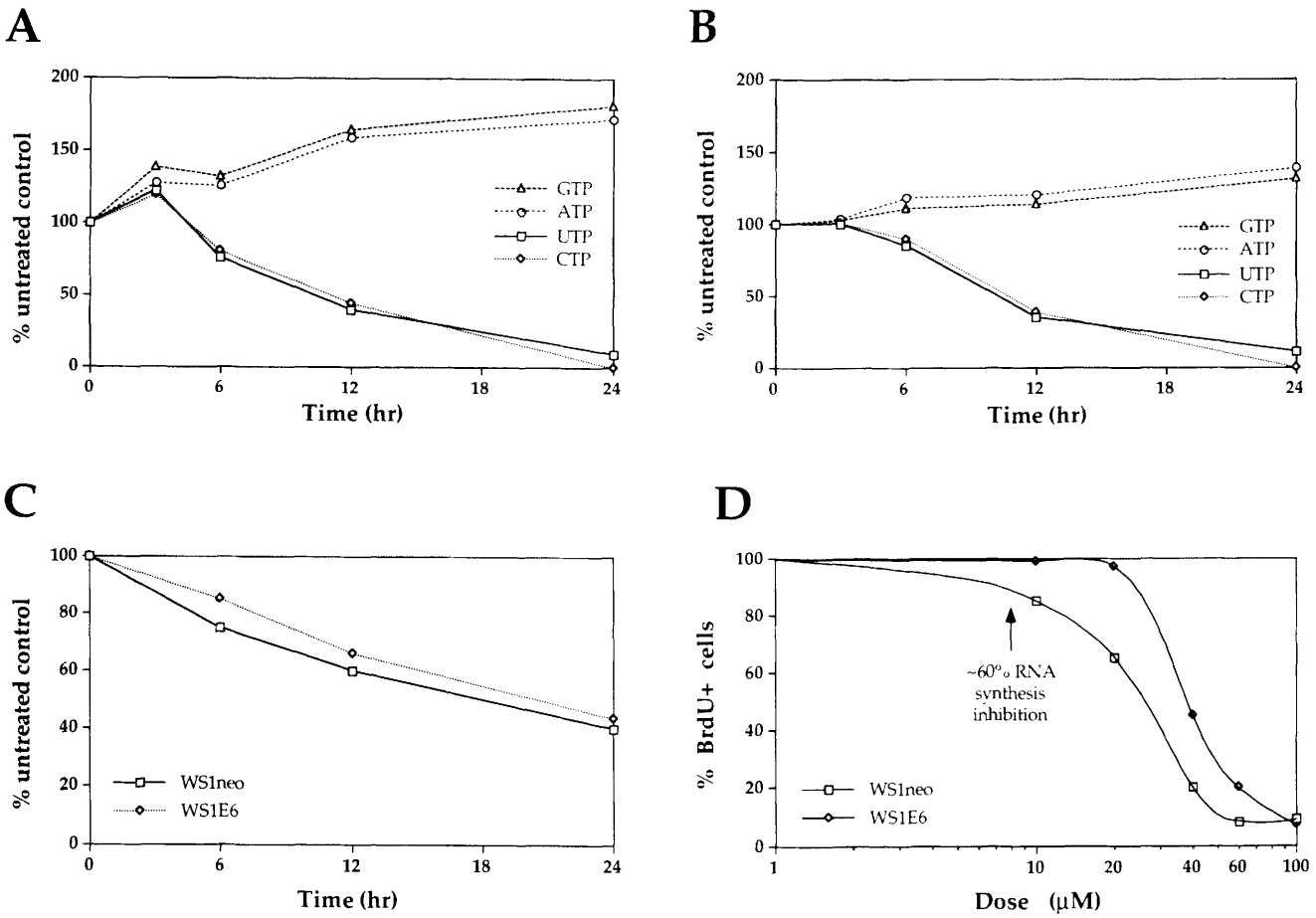

Figure 5. Effects of PALA on rNTP levels and RNA synthesis rates, and effects of DRB on cell cycle progression. Cells were treated with 100 μM PALA and harvested between 3 and 24 hr later to determine rNTP levels by HPLC in WS1neo (*A*) and WS/E6 (*B*), and overall RNA synthesis rates in both cell strains (*C*). (*D*) G_0-synchronized cells were treated with the indicated concentrations of the RNA synthesis inhibitor DRB upon release in the presence of BrdU, and the percentage of BrdU-labeled cells was determined after 72 hr. ↑ Dose that inhibits RNA synthesis by ~60%. All values shown represent percentages of the untreated control.

not shown). These data confirm that all of the drugs exhibited the expected effects on nucleotide metabolism regardless of p53 status.

Inhibition of RNA synthesis does not correlate with the PALA-induced, p53-dependent G_1 arrest

We tested whether the antimetabolites failed to arrest $p53^-$ cells because of differences in the magnitude of RNA synthesis inhibition compared to $p53^+$ cells, and whether RNA synthesis inhibitors caused a p53-dependent arrest. WS1neo and WS1E6 cells were treated with 100 μM PALA for 6, 12, and 24 hr, and RNA synthesis rates were determined by incorporation of [^{3}H]guanosine during a 1-hr pulse to verify that synthesis rates were affected similarly in both cell types ([^{3}H]guanosine was used as the tracer, as guanosine pools are not affected by PALA treatment). Rates of synthesis were reduced moderately, to ~40% of control, in both WS1neo and WS1E6 cells by 24 hr, suggesting that PALA inhibits RNA synthesis similarly in both cell types (Fig. 5C). Comparable results were obtained for uninfected WS1 cells ($p53^+$) and LFS-041 cells (no p53 expression) (data not shown).

We also determined whether inhibition of RNA polymerase II could elicit a p53-dependent arrest. Treatment of G_0-synchronized cells released in 5,6-dichloro-1-β-D-ribofuranosylbenzimidazole (DRB) caused a dose-dependent G_0/G_1 arrest in both $p53^+$ and $p53^-$ cells (Figure 5D). Similar results were acheived with α-amanitin and in asynchronous cultures. Although somewhat higher percentages of $p53^+$ cells arrested at each dose, little arrest was seen during treatment with DRB at doses that inhibited RNA synthesis to the same degree as that caused during PALA-induced arrest (~60% inhibition; indicated in Fig. 5D). These findings suggest that reducing RNA synthesis by rNTP depletion does not underlie the p53-dependent arrest achieved by antimetabolites such as PALA.

Chromosomal aberrations are not detected after treatment with PALA

The sensitivity of the p53 arrest pathway raises the possibility that ribonucleotide biosynthesis inhibitors could keep G_0/G_1 cells arrested by generating DNA damage or inhibiting repair. Therefore, we estimated the ability of PALA to induce DNA damage in cells proceeding through one S phase, where inhibition of nucleotide metabolism would be most likely to produce DNA damage. G_0-synchronized WS1neo cells were released for 12 hr, allowing commitment to S phase, and then treated with 100 μM PALA and 0.1 μg/ml of colcemid for 24 hr to arrest them in metaphase. Of 96 metaphase spreads analyzed, none contained chromosomal aberrations. In addition, asynchronous NHF-3 cells were treated for 24–72 hr with 100 μM PALA and arrested in metaphase with colcemid during the final 24 hr. Only 1 out of 600 metaphases contained an aberration. The chromosomal abnormality scored was a chromatid exchange, suggesting that the initial break occurred during S phase. In contrast, ~30% of NHF-3 cells contained aberrant chromosomes after treatment with 4 Gy γ radiation (Di Leonardo et al. 1994). These data indicate that PALA treatment of cells during transit through one cell cycle does not readily induce DNA damage detectable by metaphase chromosome analysis. Therefore, it is reasonable to infer that PALA treatment would not generate DNA damage in G_0/G_1-arrested cells.

Effects of PALA and γ radiation on cell cycle regulators in asynchronous cells

Because differences were observed between the γ radiation- and antimetabolite-induced p53-dependent G_0/G_1 arrest responses, we sought to determine whether there were any differences in the effects on putative factors in the p53 arrest pathway. Asynchronous WS1neo and WS1E6 cells were treated with 100 μM PALA or 4 Gy γ radiation and harvested 6–96 hr later to determine the consequences on p53, p21, and pRb (Fig. 6A). In PALA-treated WS1neo cells, p53 was induced within 12 hr, reached a maximum of approximately fourfold above the level of the untreated control within 24 hr, and remained high through 96 hr. p21 levels were also induced within 12 hr and continued increasing through 96 hr to ~10-fold. A corresponding increase in p21 mRNA was also observed (data not shown). Dephosphorylation of pRb occurred over the time course, with noticeable conversion beginning within 12 hr. Complete conversion to the hypophosphorylated form had occurred by 48 hr (data not shown) and was sustained through 96 hr, consistent with the G_0/G_1 arrest.

The p53 level in γ-irradiated WS1neo cells underwent an early induction of about twofold (within 6 hr), declined to near baseline level, and increased again through 96 hr. We consistently observe this biphasic p53 induction in NDF. p21 protein levels increased between 6 and 12 hr after treatment and remained high (roughly sevenfold) through 96 hr. p21 mRNA levels also remained high through 96 hr (data not shown). These results are consistent with previous findings in uninfected WS1 cells (Di Leonardo et al. 1994). In line with the G_0/G_1 arrest induced by γ radiation, dephosphorylation of pRb began within 12 hr, was nearly complete by 24 hr, and was maintained through 96 hr.

Consistent with their failure to arrest, WS1neo cells cotreated with 100 μM PALA and 50 μM uridine showed little difference in p53, p21, or pRb from the untreated control over the time course (data shown only for 24 hr). In addition, WS1E6 cells treated with PALA or γ radiation contained undetectable levels of p53 and p21 and showed little or no dephosphorylation of pRb. Thus, in asynchronous cultures, p53 and p21 were induced and pRb was dephosphorylated only in treatments that led to a G_0/G_1 arrest.

Differential effects of MTX vs. PALA and γ radiation on cell cycle regulators in G_0-synchronized cells

The biochemical effects on the p53 arrest pathway were

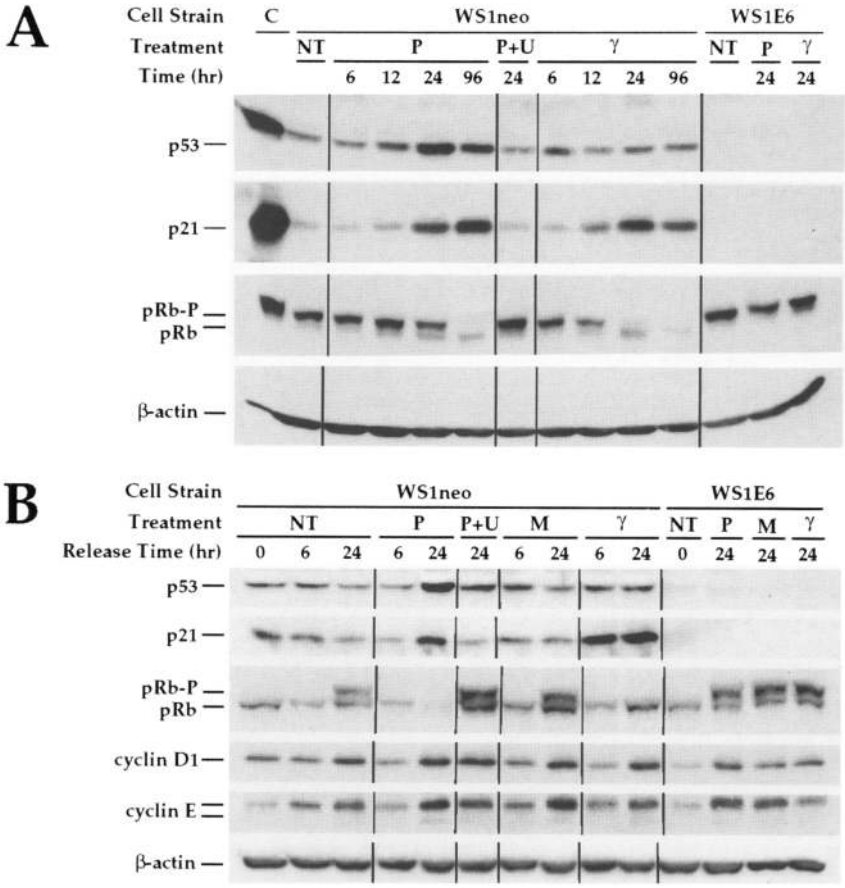

Figure 6. Immunoblot analysis of $p53^+$ and $p53^-$ cells following treatment with anticancer agents. WS1neo and WS1E6 cells were treated with 100 μM PALA (P), 100 μM PALA with 50 μM uridine (P+U), 4 Gy γ radiation, 200 nM MTX (M), or they were left untreated (NT). β-Actin is shown as a loading control. (*A*) Asynchronous cells; (*B*) Cells synchronized in G_0 by contact inhibition.

also determined in G_0-synchronized cells to eliminate the contribution of DNA damage induced by antimetabolites. Contact-inhibited WS1neo and WS1E6 cells were treated with 200 nM MTX, which allowed cells to progress into early S, or 100 μM PALA or 4 Gy γ radiation, which kept cells arrested in G_0/G_1. Cells were harvested 0, 6, 24, and 48 hr after release (Fig. 6B; data not shown). In the unreleased cultures, p21 levels were relatively high, cyclin D1 and E levels were relatively low, and pRb was in the hypophosphorylated form, consistent with previous results (e.g., Dulic et al. 1994; Noda et al. 1994). p53 and p21 were induced in WS1neo samples treated with PALA or γ radiation but not in untreated samples or those treated with MTX. Induction occurred more rapidly in γ-irradiated cells than in PALA-treated cells. Consistent with p53 and p21 levels, pRb was converted to the hyperphosphorylated form between 6 and 24 hr in the untreated and MTX-treated samples. pRb remained in the hypophosphorylated form in PALA-treated and γ-irradiated cells.

WS1neo cells cotreated with 100 μM PALA and 50 μM uridine showed little difference in p53, p21, or pRb from the untreated control over the time course. As in the asynchronous cultures, WS1E6 cells contained very low levels of p53 and p21, and pRb was phosphorylated after release regardless of the treatment (data shown only for 24 hr). Cyclin D1 and cyclin E levels increased in both cell types regardless of treatment, consistent with previous observations after γ irradiation (Dulic et al. 1994). Somewhat surprisingly, the induction of the cyclins was even more pronounced in the antimetabolite-treated samples at 24 hr and 48 hr (Fig. 6B; data not shown). Results in serum-deprived cells were similar to those in contact-inhibited cells, except that initial p53 levels were higher and p21 levels were lower in the serum-deprived samples and p21 showed a slight induction following release in complete medium (data not shown). These results are consistent with the finding that release of G_0-synchronized cells in MTX enabled them to progress through G_1 and arrest in late G_1 or early S phase independent of p53 status, whereas γ radiation or PALA treatment maintained the arrest in G_0/G_1 dependent on p53.

Discussion

The data in this report demonstrate that p53 is part of a sensing mechanism that mediates a G_0/G_1 arrest in response to ribonucleotide biosynthesis inhibitors. It is unlikely that the metabolic depletion caused by such drugs causes arrest by inducing DNA damage because (1) the arrest is reversible upon addition of the limiting nucleotide, (2) it occurs in cells that have not undergone DNA replication or that contain detectable DNA damage, and

(3) it is specific for rNTP depletion. These observations lead us to propose that NDF, and probably other cell types, possess a previously undescribed p53-dependent arrest pathway triggered by ribonucleotide pool depletion by antimetabolites such as PALA, Pyf, CPEC, MA, and TF in the absence of DNA damage.

The reversibility of the arrest induced by the antimetabolites contrasts with the prolonged or permanent arrest induced in NDF by γ radiation (Di Leonardo et al. 1994). The longevity of the damage-induced arrest, the sustained induction of p21 (Noda et al. 1994), and the greatly enlarged and flattened cellular morphology led us to propose that DNA damage induces a senescent-like state in NDF (Di Leonardo et al. 1994). This irreversible arrest could arise from the presence of one or more irreparable DNA breaks, which would provide a constant arrest signal to p53. In contrast, the ribonucleotide depletion-associated arrest resembles quiescence in that it is readily reversed by addition of a metabolite required for growth, cells reenter S phase at about the same time as cells released from serum deprivation or contact inhibition, and cells do not undergo profound morphological changes. However, we note that elevated cyclin levels distinguishes the antimetabolite-induced arrest from quiescence, and although hypophosphorylated pRb is probably one factor in the arrest, other factors downstream of p53 may also be involved.

The arrest induced in NDF by ribonucleotide depletion did not require transit through S phase or any apparent G_0/G_1 DNA damage. The agents were nearly as effective as contact inhibition or serum deprivation at preventing cells from progressing into S phase. Greater than 90% of G_0-synchronized cells released in PALA or Pyf remained arrested in the initial G_0/G_1. Such an arrest would be equivalent to treating these cells with ~12 Gy of γ radiation (S. Linke, unpubl.). At this level of radiation, we would expect ~90% of cells to contain detectable chromosomal aberrations based on previous observations (Di Leonardo et al. 1994). However, we observed a frequency of only 0.14% (one chromatid exchange in 696 metaphases) after treatment of NDF with PALA for approximately one cell cycle.

It has been reported that DNA damage occurs during PALA treatment of asynchronous ML-1 myeloid leukemia cells (which contain wild-type p53), leading to the suggestion that like γ radiation, antimetabolites cause arrest by inducing damage (Nelson and Kastan 1994). However, we found that ML-1 cells do not arrest in G_1 like NDF during PALA treatment but, rather, continue into and through S phase and undergo apoptosis (A. Di Leonardo and S. Linke, unpubl.). Thus, data from ML-1 may not be concordant with other cell types.

It is possible that ribonucleotide depletion during G_0/G_1 might inhibit repair of endogenous DNA damage, either by reducing the required dNTP precursors or by interfering with transcription or transcription-coupled repair. If this were the case, other nucleotide biosynthesis inhibitors would also be expected to inhibit repair and induce a p53-dependent arrest. However, the dNTP biosynthesis inhibitors HU, 5-FU, and MTX, which are more potent inhibitors of dNTP synthesis, did not affect the transit of either $p53^+$ or $p53^-$ cells through G_1, as both cell types progressed into early S phase from G_0 synchrony. Unlike cells treated with PALA, cells treated with MTX showed phosphorylation of pRb after release from G_0 synchrony, further indicating their ability to progress through G_1. Furthermore, although nucleotide depletion might inhibit repair, it should not prevent it, as low levels of nucleotides are always present even in the presence of the inhibitors. Yet cells remained arrested in G_0/G_1 for at least 96 hr in this study and have been shown to stay arrested for several weeks (Livingstone et al. 1992; Di Leonardo et al. 1993b). Taken together, these data indicate that the specificity of the p53-dependent arrest for certain ribonucleotide biosynthesis inhibitors is unlikely to be attributable to inhibition of repair of DNA damage.

The signal transduction pathways that lead to G_0/G_1 arrest when DNA damage is present or ribonucleotide pools are depleted appear similar. However, subtle differences are evident that may suggest the involvement of some unique components. For example, although the γ radiation-induced increase in p53 was reproducibly biphasic in $p53^+$ NDF, the increase was continuous and consistently higher after treatment with PALA. Treatment with either γ radiation or PALA caused p53-dependent increases in p21. However, whereas $p21^{-/-}$ and $p53^{-/-}$ MEFs both lose the capacity to arrest in PALA, $p21^{-/-}$ MEFs retain a partial ability to arrest after γ irradiation relative to $p53^{-/-}$ MEFs (Deng et al. 1995). These data further support the proposal that p53 responds differentially to direct DNA-damaging agents and antimetabolites.

Although antimetabolites like PALA deplete nucleotide pools, they do not prevent induction of a variety of cell cycle regulators. For example, the induction of p21 protein in $p53^+$ cells during treatment with PALA was associated with a corresponding increase in p21 mRNA (data not shown). Interestingly, the levels of certain proteins involved in cell cycle progression (cyclins D1 and E) were also elevated in both $p53^+$ and $p53^-$ cells. The highly induced levels of the Cdk inhibitor p21 in $p53^+$ cells probably helped overcome the proliferative signal of the cyclins, whereas the low basal p21 levels in $p53^-$ cells was apparently insufficient to cause arrest.

The specific signal that initiates the p53-dependent arrest described here awaits elucidation. Our results appear to be inconsistent with studies suggesting that p53 mediates the G_1 arrest by reducing GTP levels through inhibition of IMP-D (Sherley 1991), because treatments that depleted UTP and/or CTP pools caused moderate increases in GTP pools, yet produced a p53-dependent arrest. The inability of $p53^-$ cells to arrest most likely derives from their inability to sense and/or transduce upstream signals generated by nucleotide depletion. Depletion of UTP, CTP, or GTP individually was sufficient to activate the p53-dependent arrest pathway. Although ATP depletion by alanosine did not cause arrest, this may have been attributable to insufficient reduction of the large endogenous ATP pool. Among the possible

transducers of an arrest signal, we consider two general alternatives to be most likely. First, because UTP, CTP, and GTP are involved in the activation of various signal transduction intermediates, p53 might sense changes in general signaling pathways. However, preliminary experiments are not consistent with this idea, as inhibiting CTP-activated signal transduction molecules by treatment with the PI_3-kinase inhibitor wortmannin did not affect cell cycle progression in a p53-dependent manner (data not shown). Although ceramide increases could potentially result from UTP depletion and lead to pRb dephosphorylation and G_0/G_1 arrest (Dbaibo et al. 1995; Jayadev et al. 1995), we found that ceramide treatment arrested both $p53^+$ and $p53^-$ cells (data not shown). We favor a second model in which G_1 arrest is caused by inhibition of synthesis of specific RNA molecules by rNTP depletion. Two intriguing candidates are 5.8S rRNA, reportedly attached to the CKII site of murine and human p53 (Fontoura et al. 1992), and 5S rRNA, reportedly associated with p53 through an interaction with MDM2 and L5 ribonucleoproteins (Marechal et al. 1994). A majority of cellular RNA is ribosomal, so depletion of rNTPs may profoundly reduce the levels of 5S and 5.8S rRNA, their association with p53, and the association of p53 with ribosomes. As a result, p53 may be redistributed from the cytoplasm to the nucleus, enabling it to regulate transcriptional activity. In addition, rNTP depletion may affect ribosome or polysome integrity and/or synthesis of proteins needed for cell cycle advance. The viability of such a model awaits demonstration of a true regulatory role for the association of p53 with rRNA.

The p53 cell cycle control pathway plays a critical role as a DNA damage and metabolite sensor and is the most frequently inactivated target in human cancer (Hollstein et al. 1991). Once able to proliferate in the presence of broken DNA or depleted nucleotide pools, the genome is rendered highly unstable and variants exhibiting gene amplification and/or other structural chromosome rearrangements can arise. We initially speculated that p53 might play a role as a sensor of dNTP precursor pools (Di Leonardo et al. 1993b). However, the data presented here and elsewhere indicate that although rNTP depletion triggers a p53-dependent G_0/G_1 arrest, dNTP reductions do not appear to be effective (Almasan et al. 1995b; Li et al. 1995). In this light, the choice of PALA as a selective agent to assess whether p53 function contributes to amplification competence was fortuitous (Livingstone et al. 1992; Yin et al. 1992). For instance, $p53^-$ cells with functional pRb arrest at the end of G_1 or the beginning of S phase during dTTP depletion and, consequently, are prevented from progressing through S phase and undergoing gene amplification (Almasan et al. 1995a). Thus, the selective condition employed, as well as genotype, are critical determinants of genetic instability.

The knowledge that crucial regulators of cell cycle control pathways exhibit high selectivity for nucleotide depletion affords the possibility of predicting sensitivity to the nucleotide biosynthesis inhibitors employed in cancer therapy. Although it has been proposed that loss of p53 function would generate cells refractory to chemotherapy attributable to loss of apoptotic capacity (Lowe et al. 1993a), our data reveal sensitivity of $p53^-$ cells to certain nucleotide biosynthesis inhibitors. In contrast, Rb-deficient human sarcomas express elevated DHFR and TS and are intrinsically resistant to MTX (Li et al. 1995). Clearly, expansion of this data base will help achieve a more rational approach to chemotherapy based on genotype.

Materials and methods

Cells and culture conditions

WS1 (embryonic skin NDF; ATCC CRL-1502), IMR-90 (fetal lung NDF; ATCC CCL-186), NHF-3 (foreskin NDF; provided by Dr. M. Cordeiro-Stone, University of North Carolina, Chapel Hill), WI-38 (embryonic lung NDF; ATCC CCL-75), and RPE-h (normal human retinal pigmented epithelial cells; provided by Cell Genesys, Inc., Foster City, CA) contain a functional p53 pathway ($p53^+$). H1299 (non-small cell lung carcinoma lacking p53 expression because of a 5′ intragenic deletion; provided by Dr. D. Carbone, University of Texas Southwestern Medical Center, Dallas), LFS-041 and LFS-087 (postcrisis Li–Fraumeni fibroblasts expressing no p53 and mutant p53, respectively; provided by Dr. M. Tainsky, University of Texas, M.D. Anderson Cancer Center, Houston), and WI-38 VA13 (SV40-transformed derivative of WI-38; ATCC CCL-75.1) are human lines with a nonfunctional p53 pathway ($p53^-$). HEC-1-A (human endometrial adenocarcinoma; ATCC HTB 112) was used as an immunoblot control for p53, p21, and pRb.

Pools of NDF and RPE-h expressing a neomycin resistance gene (neo; $p53^+$) or expressing neomycin resistance and the oncogenic human papillomavirus type 16 E6 protein (E6; $p53^-$) were prepared by retroviral gene transduction as described in Halbert et al. (1992) using murine PA317 producer lines (provided by Dr. D. Galloway, Fred Hutchinson Cancer Research Center, Seattle, WA). Cells expressing E6 have a nonfunctional p53 pathway, as E6 directs the degradation of p53 by ubiquitination (Scheffner et al. 1990). Immunoblot analysis revealed that pools expressing neo and E6 (WS1E6, NHF-3E6, WI-38E6, and RPE-hE6) contained extremely low, almost undetectable, levels of p53 relative to pools expressing neo only (WS1neo, NHF-3neo, WI-38neo, and RPE-hneo) (data not shown).

All cell strains and lines, except the neo and E6 pools and RPE-h, were maintained in Earle's minimal essential medium supplemented with 1× nonessential amino acids (GIBCO) and 10% dialyzed fetal bovine serum (dFBS; Sigma). The neo and E6 pools were maintained as above with the addition of 400 μg/ml of G-418 sulfate. RPE-h pools were maintained in a 1:1 mix of Dulbecco's modified Eagle medium and F12 medium (GIBCO) supplemented with 10% dFBS. All cells were grown at 37°C in a humidified atmosphere containing 7% CO_2. Cells were split 1:5 approximately every 3 days at ~70% confluence for maintenance.

Chemicals and γ irradiation

α-amanitin, BrdU, DRB, 5-FU (NSC-19893), guanine, HU (NSC-32065), hypoxanthine, MA (NSC-129185), MMPR (NSC-40774), thymidine, uridine, and xanthine were obtained from Sigma. THU was obtained from Calbiochem (San Diego, California). Alanosine (NSC-153353), CPEC (NSC 375575), MTX (NSC-740), PALA (NSC-224131), (Pyf; NSC-143095), and TF (NSC-286193) were provided by the Drug Biosynthesis & Chemistry Branch, Developmental Therapeutics Program, Division of

Cancer Treatment, National Cancer Institute (Bethesda, MD). Cells were treated with γ radiation at room temperature with a ^{60}Co γ-irradiator (Gammabeam 150-C) at a distance of 40 cm and a rate of ~3.8 Gy/min (1 Gy = 100 rads).

Flow cytometric cell cycle analysis

For experiments on asynchronous cultures, cells were seeded 24 hr prior to treatment at densities to prevent contact inhibition. Cultures were pulse-labeled with 10 μM BrdU (a thymidine analog) for 30 min 24–72 hr after treatment, harvested, and subjected to flow cytometric cell cycle analysis as described below. Experiments were repeated a minimum of two times. G_0 synchrony was achieved by two different methods, contact inhibition or serum deprivation. For experiments on contact-inhibited cultures, cells were held at confluency for 48 hr and released by replating at a lower density (1:3 to 1:5). For experiments on serum-deprived cultures, the dFBS concentration in the medium was reduced from 10% to 0.1% for 48 hr, and cells were released in medium containing 10% dFBS. BrdU (65 μM) was added at the time of release for continuous labeling of cells undergoing DNA synthesis (except as otherwise noted). Tissue culture dishes were wrapped in aluminum foil for continuous labeling experiments to minimize light-induced DNA breakage. Cultures were harvested and subjected to flow cytometric cell cycle analysis 48–96 hr after release as described below. Experiments were repeated a minimum of two times.

After harvest by trypsinization, cells were fixed in 70% ethanol until the day of analysis. Cells were treated with 0.1 M HCl containing 0.5% Triton X-100 to extract histones, followed by boiling and rapid cooling to denature the DNA. Cells were then incubated with anti-BrdU–FITC (Pharmingen, San Diego, CA) and counterstained with propidium iodide containing RNase. Samples were run on a Becton-Dickinson FACScan using color compensation when appropriate. Data analysis was done using SunDisplay3 (J. Trotter, Salk Institute Flow Cytometry Lab, La Jolla, CA). Cellular debris and fixation artifacts were gated out, and the G_0/G_1, S, and G_2/M fractions were quantified.

Immunofluoresence staining

WS1neo cells were seeded on coverslips in 6-cm tissue culture dishes and treated with either 100 μM PALA or 4 Gy γ radiation. Cells were fixed for 2 min in methanol/acetone (1:1) at −20°C after treatment for 3, 12, 24, and 96 hr. Fixed cells were stored in PBSAT (phosphate-buffered saline containing 0.1% BSA, 0.02% NaN_3, and 0.2% Triton X-100) at 4°C until the samples from all time points were collected. Cells were blocked in PBS–BSA (phosphate-buffered saline containing 3% BSA and 0.02% NaN_3) and stained with mouse mAb anti-p53 DO-1 (Ab-6; Santa Cruz Biotechnology, Santa Cruz, CA) at 4°C overnight. Excess antibody was removed by washing with PBSAT three times. Cells were subsequently labeled with fluorescein isothiocyanate-conjugated anti-mouse antibody at room temperature for 1 hr. After extensive washes in PBSAT, stained cells were photographed under 100× magnification.

Metaphase aberration assay

Cells (2×10^6) were seeded in 75-cm^2 flasks and treated as indicated. Cultures were then incubated in 0.1 μg/ml of colcemid (GIBCO) for 24 hr, and mitotic cells were harvested. Cells were swollen for 10 min in 75 mM KCl at 37°C, fixed with three changes of methanol/acetic acid (3:1), and dropped onto clean glass microscope slides. Slides were stained in 2.5% Giemsa for 10 min, and metaphase spreads were scored for chromatid breaks, chromatid exchanges, chromosome exchanges (dicentrics), and double minutes using a Zeiss microscope under a 100× objective lens (Savage 1976; Di Leonardo et al. 1993a).

rNTP pool and RNA biosynthesis analyses

rNTP analysis was done as described in Pogolotti and Santi (1982). A total of 5×10^6 cells were seeded in two 15-cm tissue culture dishes 24 hr prior to treatment, treated with the desired drug, and harvested at the indicated time points. Proteins, DNA, and RNA were precipitated with 10% TCA, and the supernatants were neutralized with 1.1 volume Freon containing 0.5 M tri-*n*-octylamine (Sigma). The neutralized extracts were analyzed by HPLC (Waters) on a Partisil 10-SAX column. TCA precipitates were solubilized in 0.3 M KOH, and protein was quantified by a modified Lowry method (Bio-Rad) for normalization.

For RNA biosynthesis rates, 5×10^5 cells were seeded 24 hr before treatment. Cells were treated as indicated and pulse-labeled for 1 hr with 1 μCi/ml of [^{3}H]guanosine (Moravek Biochemicals, Brea, CA) at the indicated time points. [^{3}H]guanosine was used as the tracer, as its levels are not affected significantly by PALA treatment. RNA, DNA, and protein were precipitated with 0.5 M $HClO_4$, and the pellet was washed twice with 0.5 M $HClO_4$ to remove free nucleotides. The RNA was then hydrolyzed in 0.3 M KOH for 30 min at 50°C. Solubilized DNA and protein were reprecipitated in 70% $HClO_4$, and radioactivity was assayed in the supernatant fraction.

Immunoblot analysis

Cells were lysed in buffer containing 3% SDS, 125 mM Tris at pH 6.7, 6% urea, and 10% glycerol with 100 μg/ml of PMSF and 60 μg/ml of aprotinin. Protein concentrations were determined by a modified Lowry method (Bio-Rad). Lysates (35 μg) were resolved by 6.5% or 10% SDS-PAGE gels and electroblotted to supported nitrocellulose membranes (Schleicher & Schuell) under standard conditions (Ausubel et al. 1994). Electroblotted gels were stained with Coomassie blue, and membranes were reversibly stained with Ponceau S to verify equal loading and transfer. Membranes were then probed with mouse mAbs anti-WAF1 (Ab-1; Oncogene Science, San Diego, CA), anti-p53 DO-1 (Ab-6; Santa Cruz Biotechnology), anti-cyclin E (HE12; Santa Cruz Biotechnology), anti-pRb 3C8 (Canji, Inc., San Diego, CA), and anti-β-actin (Sigma), and rabbit polyclonal antibody anti-cyclin D1 (W. Jiang, unpubl.). Detection was done by ECL according to manufacturer's instructions (DuPont NEN), and quantification was done by computer scan densitometry (NIH Image). Experiments were repeated at least twice.

Acknowledgments

We thank Drs. Gerry Boss, Robert Carroll, John Kolman, Stephen O'Gorman, Alexis Traynor-Kaplan, and Mr. Tom Paulson for insightful discussions. We also thank Dr. Walter Eckhart for his insights and support of A.T., and Dr. Gerry Boss for assistance with rNTP analysis. This work was supported by the National Cancer Institute, the Department of Defense, and the G. Harold and Leila Y. Mathers Charitable Foundation. S.P.L. was supported, in part, by a fellowship from the H.A. and Mary K. Chapman Charitable Trust. A.D.L. was supported, in part, by a special fellowship from Associazione Italiana per la Ricerca sul Cancro (FIRC).

The publication costs of this article were defrayed in part by payment of page charges. This article must therefore be hereby

marked "advertisement" in accordance with 18 USC section 1734 solely to indicate this fact.

References

Almasan, A., S. Linke, T. Paulson, L.-C. Huang, and G. Wahl. 1995a. Genetic instability as a consequence of inappropriate entry and progression through S-phase. *Cancer Metastasis Rev.* **14:** 59–73.

Almasan, A., Y. Yin, R.E. Kelly, E.Y. Lee, A. Bradley, and G.M. Wahl. 1995b. pRb deficiency leads to inappropriate entry into S phase, activation of E2F responsive genes and apoptosis. *Proc. Natl. Acad. Sci.* **92:** 5436–5440.

Ausubel, F.M., R. Brent, R.E. Kingston, D.D. Moore, J.G. Seidman, J.A. Smith, and K. Struhl. 1994. *Current protocols in molecular biology*, Vol. 2, p. 10.2. Wiley/Greene, New York, NY.

Bertoni, L., C. Attolini, L. Tessera, E. Mucciolo, and E. Giulotto. 1994. Telomeric and nontelomeric (TTAGGG)n sequences in gene amplification and chromosome stability. *Genomics* **24:** 53–62.

Bodner, S.M., J.D. Minna, S.M. Jensen, D. D'Amico, D. Carbone, T. Mitsudomi, J. Fedorko, D.L. Buchhagen, M.M. Nau, A.F. Gazdar et al. 1992. Expression of mutant p53 proteins in lung cancer correlates with the class of p53 gene mutation. *Oncogene* **7:** 743–749.

Cadman, E. and C. Benz. 1980. Uridine and cytidine metabolism following inhibition of de novo pyrimidine synthesis by pyrazofurin. *Biochim. Biophys. Acta* **609:** 372–382.

Cadman, E.C., D.E. Dix, and R.E. Handschumacher. 1978. Clinical, biological, and biochemical effect of pyrazofurin. *Cancer Res.* **38:** 682–688.

Clarke, A.R., C.A. Purdie, D.J. Harrison, R.G. Morris, C.C. Bird, M.L. Hooper, and A.H. Wyllie. 1993. Thymocyte apoptosis induced by p53-dependent and independent pathways. *Nature* **362:** 849–852.

Cohen, M.B. and W. Sadee. 1983. Contributions of the depletions of guanine and adenine nucleotides to the toxicity of purine starvation in the mouse T lymphoma cell line. *Cancer Res.* **43:** 1587–1591.

Collins, K.D. and G.R. Stark. 1971. Aspartate transcarbamylase. Interaction with the transition state analogue N-(phosphonacetyl)-L-aspartate. *J. Biol. Chem.* **246:** 6599–6605.

Cooney, D.A., H.N. Jayaram, G. Gebeyehu, C.R. Betts, J.A. Kelley, V.E. Marquez, and D.G. Johns. 1982. The conversion of 2-beta-D-ribofuranosylthiazole-4-carboxamide to an analogue of NAD with potent IMP dehydrogenase-inhibitory properties. *Biochem. Pharmacol.* **31:** 2133–2136.

Dbaibo, G.S., M.Y. Pushkareva, S. Jayadev, J.K. Schwarz, J.M. Horowitz, L.M. Obeid, and Y.A. Hannun. 1995. Retinoblastoma gene product as a downstream target for a ceramide-dependent pathway of growth arrest. *Proc. Natl. Acad. Sci.* **92:** 1347–1351.

Deng, C., P. Zhang, J.W. Harper, S.J. Elledge, and P. Leder. 1995. Mice lacking $p21^{CIP1/WAF1}$ undergo normal development, but are defective in G_1 checkpoint control. *Cell* **82:** 675–684.

Di Leonardo, A., P. Cavolina, and A. Maddalena. 1993a. DNA topoisomerase II inhibition and gene amplification in V79/B7 cells. *Mutat. Res.* **301:** 177–182.

Di Leonardo, A., S.P. Linke, Y. Yin, and G.M. Wahl. 1993b. Cell cycle regulation of gene amplification. *Cold Spring Harbor Symp. Quant. Biol.* **58:** 655–667.

Di Leonardo, A., S.P. Linke, K. Clarkin, and G.M. Wahl. 1994. DNA damage triggers a prolonged p53-dependent G_1 arrest and long-term induction of Cip1 in normal human fibroblasts. *Genes & Dev.* **8:** 2540–2551.

Dulic, V., W.K. Kaufmann, S.J. Wilson, T.D. Tlsty, E. Lees, J.W. Harper, S.J. Elledge, and S.I. Reed. 1994. p53-dependent inhibition of cyclin-dependent kinase activities in human fibroblasts during radiation-induced G_1 arrest. *Cell* **76:** 1013–1023.

El-Deiry, W.S., J.W. Harper, P.M. O'Connor, V.E. Velculescu, C.E. Canman, J. Jackman, J.A. Pietenpol, M. Burrell, D.E. Hill, Y. Wang, K.G. Wiman, W.E. Mercer, M.B. Kastan, K.W. Kohn, S.J. Elledge, K.W. Kinzler, and B. Vogelstein. 1994. WAF1/CIP1 is induced in p53-mediated G_1 arrest and apoptosis. *Cancer Res.* **54:** 1169–1174.

Farnham, P.J., J.E. Slansky, and R. Kollmar. 1993. The role of E2F in the mammalian cell cycle. *Biochim. Biophys. Acta* **1155:** 125–131.

Fontoura, B.M., E.A. Sorokina, E. David, and R.B. Carroll. 1992. p53 is covalently linked to 5.8S rRNA. *Mol. Cell. Biol.* **12:** 5145–5151.

Gale, G.R. and G.B. Schmidt. 1968. Mode of action of alanosine. *Biochem. Pharmacol.* **17:** 363–368.

Halbert, C.L., G.W. Demers, and D.A. Galloway. 1992. The E6 and E7 genes of human papillomavirus type 6 have weak immortalizing activity in human epithelial cells. *J. Virol.* **66:** 2125–2134.

Harper, J.W., G.R. Adami, N. Wei, K. Keyomarsi, and S.J. Elledge. 1993. The p21 Cdk-interacting protein Cip1 is a potent inhibitor of G_1 cyclin-dependent kinases. *Cell* **75:** 805–816.

Henderson, J.F. and A.R.P. Patterson. 1973. *Nucleotide metabolism: An introduction*. p. 48. Academic Press, New York, NY.

Hollstein, M., D. Sidransky, B. Vogelstein, and C.C. Harris. 1991. p53 mutations in human cancers. *Science* **253:** 49–53.

Huang, L.-C., K.C. Clarkin, and G.M. Wahl. 1996. Sensitivity and selectivity of the p53-mediated DNA damage sensor. *Proc. Natl. Acad. Sci.* (in press).

Hupp, T.R., A. Sparks, and D.P. Lane. 1995. Small peptides activate the latent sequence-specific DNA binding function of p53. *Cell* **83:** 237–245.

Ishizaka, Y., M.V. Chernov, C.M. Burns, and G.R. Stark. 1995. p53-dependent growth arrest of REF52 cells containing newly amplified DNA. *Proc. Natl. Acad. Sci.* **92:** 3224–3228.

Jayadev, S., B. Liu, A.E. Bielawska, J.Y. Lee, F. Nazaire, M. Pushkareva, L.M. Obeid, and Y.A. Hannun. 1995. Role for ceramide in cell cycle arrest. *J. Biol. Chem.* **270:** 2047–2052.

Kastan, M.B., O. Onyekwere, D. Sidransky, B. Vogelstein, and R.W. Craig. 1991. Participation of p53 protein in the cellular response to DNA damage. *Cancer Res.* **51:** 6304–6311.

Kastan, M.B., Q. Zhan, W.S. El-Deiry, F. Carrier, T. Jacks, W.V. Walsh, B.S. Plunkett, B. Vogelstein, and A.J. Fornace. 1992. A mammalian cell cycle checkpoint pathway utilizing p53 and GADD45 is defective in ataxia-telangiectasia. *Cell* **71:** 587–597.

Kuerbitz, S.J., B.S. Plunkett, W.V. Walsh, and M.B. Kastan. 1992. Wild-type p53 is a cell cycle checkpoint determinant following irradiation. *Proc. Natl. Acad. Sci.* **89:** 7491–7495.

Kuo, M.T., R.C. Vyas, L.X. Jiang, and W.N. Hittelman. 1994. Chromosome breakage at a major fragile site associated with P-glycoprotein gene amplification in multidrug-resistant CHO cells. *Mol. Cell. Biol.* **14:** 5202–5211.

Li, W., J. Fan, D. Hochhauser, D. Banerjee, Z. Zielinski, A. Almasan, Y. Yin, R. Kelly, G.M. Wahl, and J.R. Bertino. 1995. Lack of functional retinoblastoma protein mediates increased resistance to antimetabolites in human sarcoma cell lines. *Proc. Natl. Acad. Sci.* **92:** 10436–10440.

Livingstone, L.R., A. White, J. Sprouse, E. Livanos, T. Jacks, and T.D. Tlsty. 1992. Altered cell cycle arrest and gene amplifi-

cation potential accompany loss of wild-type p53. *Cell* **70:** 923–935.

Lowe, S.W., H.E. Ruley, T. Jacks, and D.E. Housman. 1993a. p53-dependent apoptosis modulates the cytotoxicity of anticancer agents. *Cell* **74:** 957–967.

Lowe, S.W., E.M. Schmitt, S.W. Smith, B.A. Osborne, and T. Jacks. 1993b. p53 is required for radiation-induced apoptosis in mouse thymocytes. *Nature* **362:** 847–849.

Ma, C., S. Martin, B. Trask, and J.L. Hamlin. 1993. Sister chromatid fusion initiates amplification of the dihydrofolate reductase gene in Chinese hamster cells. *Genes & Dev.* **7:** 605–620.

Marechal, V., B. Elenbaas, J. Piette, J.C. Nicolas, and A.J. Levine. 1994. The ribosomal L5 protein is associated with mdm-2 and mdm-2-p53 complexes. *Mol. Cell. Biol.* **14:** 7414–7420.

Moran, R.G., M. Mulkins, and C. Heidelberger. 1979. Role of thymidylate synthetase activity in development of methotrexate cytotoxicity. *Proc. Natl. Acad. Sci.* **76:** 5924–5928.

Moyer, J.D., P.A. Smith, E.J. Levy, and R.E. Handschumacher. 1982. Kinetics of N-(phosphonacetyl)-L-aspartate and pyrazofurin depletion of pyrimidine ribonucleotide and deoxyribonucleotide pools and their relationship to nucleic acid synthesis in intact and permeabilized cells. *Cancer Res.* **42:** 4525–4531.

Moyer, J.D., N.M. Malinowski, S.P. Treanor, and V.E. Marquez. 1986. Antitumor activity and biochemical effects of cyclopentenyl cytosine in mice. *Cancer Res.* **46:** 3325–3329.

Nasmyth, K. 1993. Control of the yeast cell cycle by the Cdc28 protein kinase. *Curr. Opin. Cell Biol.* **5:** 166–179.

Nelson, W.G. and M.B. Kastan. 1994. DNA strand breaks: The DNA template alterations that trigger p53-dependent DNA damage response pathways. *Mol. Cell. Biol.* **14:** 1815–1823.

Noda, A., Y. Ning, S.F. Venable, O.M. Pereira-Smith, and J.R. Smith. 1994. Cloning of senescent cell-derived inhibitors of DNA synthesis using an expression screen. *Exp. Cell Res.* **211:** 90–98.

Pogolotti, A.J. and D.V. Santi. 1982. High-pressure liquid chromatography–ultraviolet analysis of intracellular nucleotides. *Anal. Biochem.* **126:** 335–345.

Santi, D.V., C.S. McHenry, and H. Sommer. 1974. Mechanism of interaction of thymidylate synthetase with 5-fluorodeoxyuridylate. *Biochemistry* **13:** 471–481.

Savage, J.R. 1976. Classification and relationships of induced chromosomal structual changes. *J. Med. Genet.* **13:** 103–122.

Scheffner, M., B.A. Werness, J.M. Huibregtse, A.J. Levine, and P.M. Howley. 1990. The E6 oncoprotein encoded by human papillomavirus types 16 and 18 promotes the degradation of p53. *Cell* **63:** 1129–1136.

Sherley, J.L. 1991. Guanine nucleotide biosynthesis is regulated by the cellular p53 concentration. *J. Biol. Chem.* **266:** 24815–24828.

Skoog, L. and B. Nordenskjold. 1971. Effects of hydroxyurea and 1-beta-D-arabinofuranosyl-cytosine on deoxyribonucleotide pools in mouse embryo cells. *Eur. J. Biochem.* **19:** 81–89.

Windle, B., B.W. Draper, Y.X. Yin, S. O'Gorman, and G.M. Wahl. 1991. A central role for chromosome breakage in gene amplification, deletion formation, and amplicon integration. *Genes & Dev.* **5:** 160–174.

Xiong, Y., G.J. Hannon, H. Zhang, D. Casso, R. Kobayashi, and D. Beach. 1993. p21 is a universal inhibitor of cyclin kinases. *Nature* **366:** 701–704.

Yin, Y., M.A. Tainsky, F.Z. Bischoff, L.C. Strong, and G.M. Wahl. 1992. Wild-type p53 restores cell cycle control and inhibits gene amplification in cells with mutant p53 alleles. *Cell* **70:** 937–948.

A reversible, p53-dependent G0/G1 cell cycle arrest induced by ribonucleotide depletion in the absence of detectable DNA damage.

S P Linke, K C Clarkin, A Di Leonardo, et al.

Genes Dev. 1996, **10:**
Access the most recent version at doi:10.1101/gad.10.8.934